Electromagnetic Modeling of Waveguides Involving Finite-Size Dielectric Regions

BARRY J. RUBIN, MEMBER, IEEE

Abstract—**A moment method is presented for handling arbitrarily shaped 2-D and 3-D waveguides that involve conductors, finite-size dielectric regions, or both. A novel procedure for modeling the dielectric allows 2-D rooftop functions to represent both the 3-D polarization current in the dielectric and the surface current on the conductors, and precludes the presence of fictitious charge within the dielectric. Examples include coaxial, microstrip, and dielectric waveguides. Numerical convergence, consistency with physical principles, and agreement with the literature are demonstrated.**

I. Introduction

In calculating the scattering or guided-wave properties for microwave structures using moment methods [1], dielectric regions must often be considered. Stratified dielectrics may be accounted for by Greens functions that involve Sommerfeld integrations [2], [3]. For dielectric regions of regular shape, modal expansions and field matching procedures may be employed [4]–[8]. Irregularly shaped regions, however, may require the use of subsectional basis functions to represent either the dielectric interfaces [9]–[12] or the dielectric volume through the polarization currents [13]–[17]. The surface formulation may involve electric currents, magnetic currents, or both and may involve matching of the electric field, the magnetic field, or some combination of the two. Because only surfaces need to be modeled, in general fewer elements are required than in a volume formulation. Though some surface formulations offer advantages over others, such as avoidance of resonances associated with cavities, none have been demonstrated for 3-D structures where conductor and dielectric regions overlap. In the volume formulation, the polarization current is represented by a suitable basis function, and since the effect of the dielectric is felt only through these currents and their subsequent testing, free-space Greens functions may be used.

In the past, 3-D pulse basis functions have often been chosen to represent the polarization current [13]–[15]. Though these functions are simple, making it easy to both physically represent the dielectric and then calculate the scattered field, in accordance with the continuity equation fictitious rectangular charges will appear at pulse interfaces where the normal-directed current varies. Such fictitious charge, especially at low frequency, may be the dominant contributor to the electric field and may introduce serious errors. For scattering problems, where the far field is of interest, such effects may not be significant [15]. For guided-wave or source-driven structures, however, the electrical parameters are more closely tied to the near field, so that one cannot be comfortable using pulse functions.

Other choices for volume basis functions may also introduce difficulties. Though the tetrahedral [16] and 3-D rooftop [17] functions do not produce fictitious charge, they are not well suited for representing surface current. To model composite structures, a second type of basis function would therefore be needed. Further, to the author's knowledge these basis functions remain unproven for guided-wave problems, having appeared only in scattering analyses.

Manuscript received August 24, 1989; revised January 25, 1990.

The author is with the IBM T. J. Watson Research Center, Yorktown Heights, NY 10598.

IEEE Log Number 9035407.

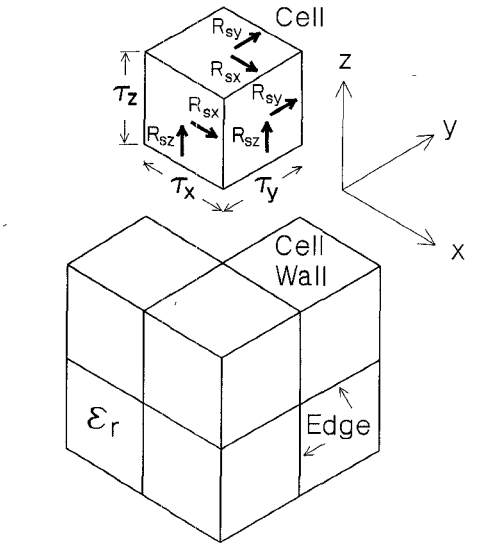

Fig. 1. Dielectric subdivision, with one cell removed for illustrative purposes.

In this paper, 2-D basis functions are used instead. The 2-D rooftop function is chosen because it is simple and sufficiently smooth, yet does not give rise to fictitious charge. We first describe how the dielectric is modeled by rooftop currents and then discuss the guided-wave formulation, with our intent to concentrate on the dielectric aspect. The versatility of the approach and numerical convergence are then demonstrated through the analysis of representative structures.

II. Modeling the Dielectric

To represent the volume polarization with surface currents, the dielectric region is first replaced by a 3-D version of the thin-wall mechanism employed by Harrington and Mautz to model dielectric shells [18]. As shown in Fig. 1, the dielectric is subdivided into sections along the Cartesian coordinates, so that the region is now composed of 3-D cells having dimensions τ_x, τ_y, and τ_z. If we conceptually push the dielectric material out from the center of each cell until it is compressed to zero thickness on the cell walls, a new structure is formed that is composed only of these zero-thickness cell walls. During compression, as the wall thickness, δ, goes to zero, the dielectric constant of the material in the wall goes to infinity as $1/\delta$. Provided the grid is sufficiently fine with respect to wavelength and feature size and provided that an appropriate sheet impedance is used to describe the cell walls, this new structure is electrically equivalent to the solid dielectric. We can therefore model composite structures having their dielectric regions so replaced, with the full expectation of obtaining equivalent electrical results. Because the cell walls have zero thickness, the currents that flow are precisely 2-D surface currents; we can represent them by rooftop functions.

This use of a basis function having fewer dimensions than the feature being modeled has analogies. For instance, wire-grid models employ 1-D basis functions to approximate 2-D surfaces [19], [20]. A 3-D grid of resistors may be used in a dc analysis to

represent a resistive volume. Such a model is actually a wire-grid representation, with the resistive material lumped into zero-radius filaments that touch at points. Based on our physical understanding and experience, if the models are properly constructed, we expect the error to vanish as the grid size is reduced. The cellular model described above, in fact, is superior to a wire-grid model [21], because the field on a surface current is well behaved while that of a line current is singular. A surface current formulation requires no fine-tuning; wire-grid formulations do, in the form of effective radii bestowed on the filaments by testing the field radially offset from their centers. As in other moment approaches, we find a satisfactory grid through numerical studies and comparisons with the literature. Many solution techniques involve grids; we just choose to apply a grid prior to the numerical solution stage.

As a practical example, consider the Teflon used in high-speed coaxial cables, which may be impregnated with air bubbles to reduce its effective dielectric constant. At typical frequencies, the dielectric appears homogeneous. After all, a material constructed with very fine cells would be difficult to detect through bulk electrical measurements. Other examples may be found in the study of artificial dielectrics.

III. Defining the Sheet Impedance

We choose a sheet impedance (or equivalently the surface impedance because the cell walls have zero thickness) such that the impedance (or capacitance) is the same between two planes that sandwich a cell of either the solid dielectric or the cellular replacement. We include only that contribution related to the volume polarization; in other words, we omit the free-space contribution [15]. From Fig. 1, the total impedance R_x along the x direction for a single cell of solid dielectric is

$$R_x = \frac{\tau_x}{j\omega\epsilon_0(\epsilon_r - 1)\tau_y\tau_z} \tag{1}$$

where ω is the angular frequency, ϵ_0 is the permittivity of free space, ϵ_r is a relative dielectric constant, and $\exp(j\omega t)$ is the time dependence. For the cellular structure, the surface impedance must be such that when multiplied by length τ_x and divided by perimeter $2(\tau_y + \tau_z)$ the result is again R_x. Thus, the surface impedance along x, R_{sx}, is given by

$$R_{sx} = \frac{2\left(\frac{1}{\tau_y} + \frac{1}{\tau_z}\right)}{j\omega\epsilon_0(\epsilon_r - 1)}. \tag{2}$$

For walls common to two cells, the impedance would be an appropriate parallel combination. Through permutation of x, y, and z, (2) also gives the surface impedances along y and z, namely R_{sy} and R_{sz}. Lossy dielectrics (or, for that matter, lossy conductor volumes) could be handled through appropriate choice of a complex permittivity.

The electric field boundary condition, applied over each dielectric cell wall and conductor surface, is

$$\boldsymbol{E} - \boldsymbol{J}_s R_s = 0 \tag{3}$$

where $\boldsymbol{E}$ is the tangential electric field, $\boldsymbol{J}_s$ is the surface current density, and R_s is the appropriate surface impedance. For dielectric volumes, R_s is either R_{sx}, R_{sy}, or R_{sz}; for perfect conductors, R_s is zero, but for imperfect conductors it may be determined through skin-effect considerations.

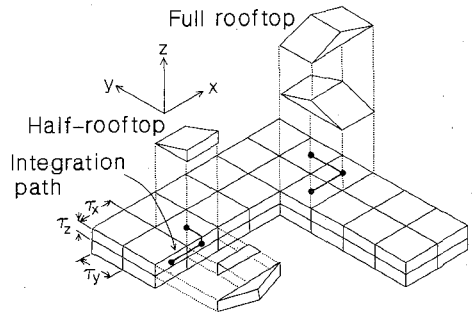

Fig. 2. A section of conductor showing full and half-rooftop elements and integration paths.

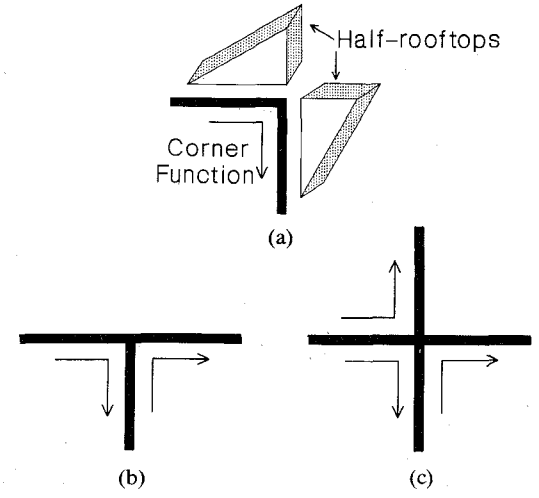

Fig. 3. Representation of junction current. (a) At external edge. (b) At three-junction. (c) At four-junction.

IV. Rooftop Representation

A rooftop function (Fig. 2), which is defined in a plane containing a surface current, has triangle dependency along the direction of current flow and pulse dependency in the transverse direction [22]–[26]. For instance, the rooftop function R, centered at the origin and corresponding to a current in the $x-y$ plane that flows along the x direction, may be expressed as

$$R = \begin{cases} 1 - \left|\dfrac{x}{\tau_x}\right|, & -\tau_x \leq x \leq \tau_x,\ -\tau_y/2 \leq y \leq \tau_y/2 \\ 0, & \text{elsewhere.} \end{cases} \tag{4}$$

For a half-rooftop, the left or right side of the inequality involving x would be replaced by 0. The charge produced by a rooftop function, from the continuity equation applied to (4), is constant over each rectangular patch it covers; by properly overlapping the rooftop functions on a surface, variations in the current flow can be represented smoothly and without producing fictitious charge.

On a dielectric or conductive surface, both full and half-rooftops (Fig. 2) may appear. To guarantee a smoother current distribution, we force the current to be continuous around bends by combining half-rooftops to form corner functions (Fig. 3(a)). Mathematically, this is accomplished by making the coefficients of associated half-rooftops equal or opposite, depending on the reference convention. This prevents the development of line charges that would yield an electric field more discontinuous than desired and would slow numerical convergence. Inter-

nal to dielectric volumes are edges, or junctions, where three or four cell walls may intersect. At an external edge, only one corner function is needed (Fig. 3(a)). At three- and four-junctions, respectively, two and three corner functions are used, as shown in parts (b) and (c) of Fig. 3. Because current flows continuously around each corner function, the total current into a junction must be zero; using more than two and three corner functions, respectively, would underspecify the current and ultimately lead to a singular matrix. The field produced by the rooftop functions must be calculated either very accurately or analytically. Otherwise, the rooftop functions may effectively become pulse functions [27] and lose their desirable properties.

At each cell edge internal to the dielectric, three corner rooftop functions appear. To represent a cell buried within the dielectric, considering that there are 12 edges per cell but that each edge is shared by four neighboring cells, nine basis functions per cell are required. This compares with only three for a wire-grid, 3-D rooftop, or 3-D pulse representation. For 2-D structures, five rooftop functions per cell are required. This disadvantage, however, will be offset by the linear fit (along one direction of the rooftop), the absence of fictitious charge, and the modeling flexibility afforded by this representation.

V. Guided-Wave Formulation

The guided-wave formulation is that already described in the literature [22]–[26], aside from the modification of R_s discussed earlier. A unit cell that includes the guided-wave structure is defined. The unit cell has periodicity d_1 along x and periodicity d_2 along y, but is finite along z. The entire unit cell, and in the present formulation this includes the dielectric regions as well, is divided into S_x, S_y, and S_z sections along the coordinate axes. With respect to Fig. 1, $S_x = d_1/\tau_x$, $S_y = d_2/\tau_y$, and S_z is the height of the unit cell divided by τ_z. The current (both conduction and polarization components) is represented as a linear combination of rooftop currents multiplied by the phase factor $\exp(jk_x x)$, where the direction of propagation is along x and k_x is the propagation constant. The electric field produced by the above distribution is found, and the electric field boundary condition (3) is then applied; it is only here that a distinction is made, through R_s, between conduction and polarization currents. Line function testing of the electric field is used to generate a matrix equation of the form

$$\boldsymbol{Z}(k_x)\boldsymbol{I} = \boldsymbol{0}. \tag{5}$$

For a current representation involving P rooftop currents, $\boldsymbol{Z}$ is an impedance matrix of order P and $\boldsymbol{I}$ is a current column vector of length P. Each element of the $\boldsymbol{Z}$ matrix relates a line integral of the electric field to a particular rooftop coefficient. Because the unit cell is periodic, each element is a Fourier-type infinite series that involves indices n and m, where n is associated with the x direction and m with the y direction. The elements are calculated analytically, with accuracy limited only by the number of terms used in the infinite series. Good results [22], [23] have been obtained when the infinite series are truncated according to $|n| \leqslant N$ and $|m| \leqslant M$, where

$$N = \frac{d_1}{\min(\tau_x, \tau_z)} \quad \text{and} \quad M = \frac{d_2}{\min(\tau_y, \tau_z)}. \tag{6}$$

Equation (5) represents an eigenvalue problem. As discussed in [24]–[26], such a problem may be solved through a Newton search and standard linear algebra techniques. In brief, values of k_x that make $\det(\boldsymbol{Z})$ vanish are found and then substituted back into (5) to obtain $\boldsymbol{I}$; the values of k_x are the eigenvalues and the corresponding values of $\boldsymbol{I}$ are the eigenvectors. Once the current distribution is found, the characteristic impedance for quasi-TEM structures may be found through appropriate integrations of the electric field. Equivalent values of capacitance and inductance may then be obtained from the impedance and propagation constant [24]. The derivation of the Z matrix elements is given in [22]. Explicit formulas for a subset of these elements are given in [24] and [25].

In the following examples, propagation is along the x direction. Rooftop current elements, as described earlier, will represent the currents in the $x-y$, $y-z$, and $x-z$ planes, with current flow along two directions in each plane. For the 2-D structures, currents appear only on the $x-z$ and $x-y$ planes and only one subdivision along x is used ($S_x = 1$); the x-directed currents will be represented only by full rooftops along the x direction. Because the x dependence of the current in 2-D structures must have the form $\exp(jk_x x)$, the infinite series will be truncated according to $N = 0$, and not N as given by (6). Although coupling between waveguides can be investigated [22]–[25], here we are concerned with isolated structures. The periodicity of the unit cell along y will be set large enough so that coupling between adjacent unit cells can be ignored. Because d_2 cannot be made infinite, some peculiarities in the solutions may occur; these will be discussed as they arise.

VI. Numerical Results

The first example, used for convergence studies, is a square coaxial cable filled with a dielectric material having $\epsilon_r = 100$. Fig. 4 shows a quarter section of the structure and gives the normalized transverse current distribution for $b/\lambda_0 = 0.00133$ and $S_y = S_z = 8$, where λ_0 is the free-space wavelength. Corner functions are used to represent the y-directed current in the $x-y$ plane and the z-directed current in the $x-z$ plane; the x-directed currents are not shown. On a cell wall, as many as four corner functions may partially overlap, as do the corner functions in Fig. 4(a) having values -766, 472, 91, and -384.

The net current flow is obtained by adding the contributions of corner functions where they overlap and is shown in Fig. 4(b). The currents shown are those just entering or leaving a junction; corresponding to the rooftop representation, the current varies linearly across a wall. Consistent with the use of corner functions, the net current is zero at all junctions. The current varies only slightly over each wall, so that here too, from the continuity equation, essentially no charge is developed. This absence of charge is expected in a homogeneous dielectric region. On the conductors, though, the currents differ and there is a net charge density. As expected, the minimum and maximum fields (and thus polarization currents) are at the outside and inside metal corners, respectively.

Though nearly perfect symmetry is observed for the polarization currents about the 45° line bisecting the quarter section, some asymmetry is observed on the conductors' surface current. This is an artifice and results from the periodicity along y but not along z that is assumed in the solution technique. As the grid becomes finer or as more Fourier series terms are used in calculating the matrix elements, this asymmetry decreases. For this example only, the M used was four times that given in (6). The x-directed currents are negligible in the dielectric but large on the conductors. Their contribution to the charge density, in either case, is small and does not alter the arguments made above.

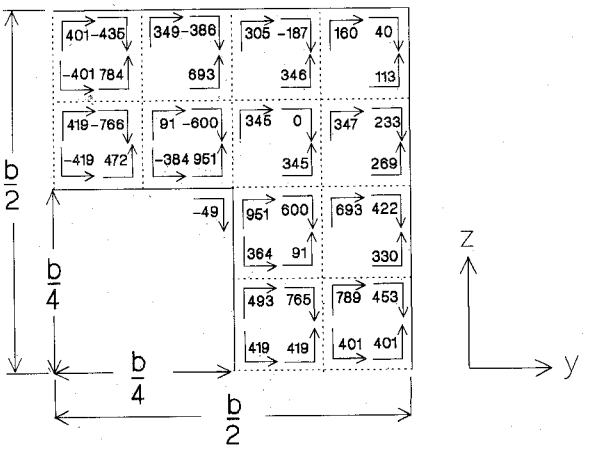

(a)

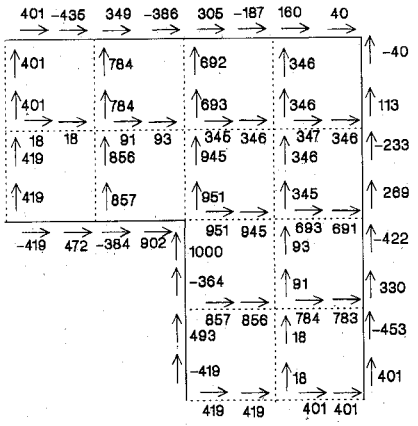

(b)

Fig. 4. Normalized current in a quarter section of the coaxial structure ($b/\lambda_0 = 0.00133$, $\epsilon_r = 100$, $S_y = S_z = 8$). (a) In terms of corner currents. (b) Net currents.

TABLE I
NORMALIZED PROPAGATION CONSTANT AND CAPACITANCE FOR COAXIAL STRUCTURE ($\epsilon_r = 100$, $b/\lambda_0 = 0.00133$)

S_y	S_z	k_x/k_0	C (pF/cm)
4	4	10.946	106.1
8	8	10.325	95.84
16	16	10.118	92.61
32	32	10.043	91.38

Because the coaxial structure is TEM, no transverse current should flow on its conductors. From Fig. 4(b), the current on the conductors alternates between positive and negative values. As the grid is made finer, such a distribution will appear on average as that of a zero current flow.

The propagation constant and the capacitance are given in Table I. For the coarsest grid ($S_y = S_z = 4$), the propagation

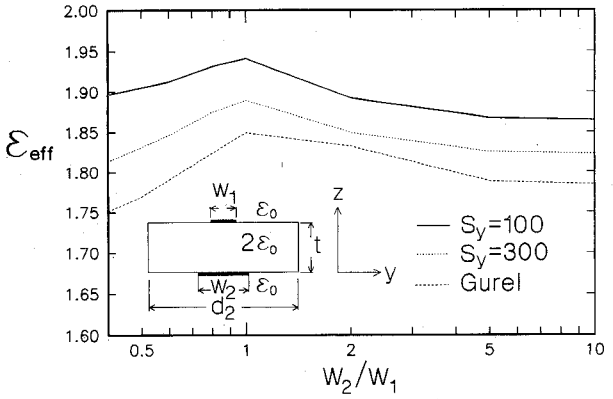

Fig. 5. Effective dielectric constant in microstrip structure ($w_1 = 0.01$ cm, $t = 0.002$ cm, $d_2 = 0.1$ cm, $f = 1.0$ GHz, $S_z = 4$).

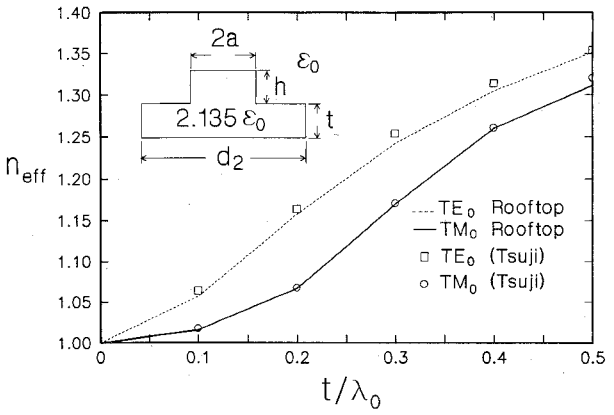

Fig. 6. Effective refractive index for ribbed waveguide ($2a/t = 1$, $h/t = 1$, $d_2/t = 16$, $S_y = 64$, $S_z = 8$).

constant normalized to the free-space wavenumber is 10.946 and the capacitance, C, is 106.1 pF/cm. As the grid is made finer along each direction by a factor of 2, the respective values monotonically approach the values of 10 (expected for a TEM structure having $\epsilon_r = 100$) and 90.49 pF/cm (calculated through a 2-D capacitance algorithm). Though moment method solutions involving the electric field are often unstable at lower frequencies [28], no instabilities were observed here despite a coaxial cross section that is only $0.00133\lambda_0$ across.

The next structure considered is a microstrip which displays an interesting peak in effective relative dielectric constant ϵ_{eff} that is not predicted from the static capacitance calculation. The effective dielectric constant at frequency $f = 1$ GHz is plotted in Fig. 5, and compared with results obtained using the approach of Gurel and Chew [3]. A grid of $S_y = 100$ and $S_z = 4$ gives agreement to within 9%. A finer but nonuniform grid (corresponding to $S_y = 300$ in the regions near conductor edges) gives agreement to within 4%. This still noticeable difference is attributed to the edge singularity. The basis functions in [3], which were carefully selected to model this particular structure, represent the edge current better than the rooftop. The above accuracies, however, are in line with moment method solutions that employ a single type of subsectional basis function.

The next structure is a ribbed dielectric waveguide (Fig. 6) having a refractive index $n_\epsilon = \sqrt{\epsilon_r} = 1.461$ and investigated by Tsuji *et al.* [6]. Since the field may not be tightly confined

(especially at larger wavelengths) significant coupling between the rib regions in adjacent unit cells may occur. This coupling is minimized by making d_2, the distance between the ribs in adjacent unit cells, substantial; in [6], d_2 is infinite. The effective refractive index, n_{eff}, is closely predicted for the lowest order modes (denoted by a 0 subscript), which in [6] are described as being essentially TE or TM to the vertical direction. Halving S_y and S_z causes only a small difference. The higher order TE and TM modes can be calculated, although their more rapid spatial variation requires that the grid be finer. In this and the following figure, the axes are normalized to be consistent with those appearing in the references.

In performing the Newton search, some difficulty was encountered. The determinant of $\mathbf{Z}$ varies, though generally monotonically, through many orders of magnitude as k_x is incrementally increased. The solution, however, occurs at a relative minimum. Though convergence is generally within four iterations once a satisfactory starting value for k_x in the Newton search is found, finding that starting point may take some effort. Another concern is that as d_2 is increased to reduce coupling, modes having lower spatial frequency along y may also satisfy the boundary conditions (as in a resonant cavity whose length increases) and this causes a splitting of the dispersion relation. For these modes, the polarization current varies sinusoidally in the region between ribs. The desired mode is identified by a generally monotonic decrease in magnitude with y distance from the rib, which is the evanescent behavior expected for a ribbed waveguide unbounded along the y direction [6].

In the last example, a square dielectric waveguide (Fig. 7) is analyzed and compared with the results reported by Goell [5]. Though the unit cell is subdivided along y into 80 sections, this corresponds to only eight sections along the dielectric region. Excellent agreement is obtained, although difficulty was again encountered in the Newton search. A similar, but hollow, structure (hollow region is $a/2$ by $a/2$ and centered) was also analyzed. A periodic array of holes is then introduced into the solid waveguide, with the first stopband plotted for the grid $S_x = 4$, $S_y = 80$, and $S_z = 8$. As expected, for wavelengths below that corresponding to the stopband (at 1.75 on the independent axis), the propagation constant falls between that for the solid and hollow cases. Near the stopband, as also expected, the curve rises dramatically.

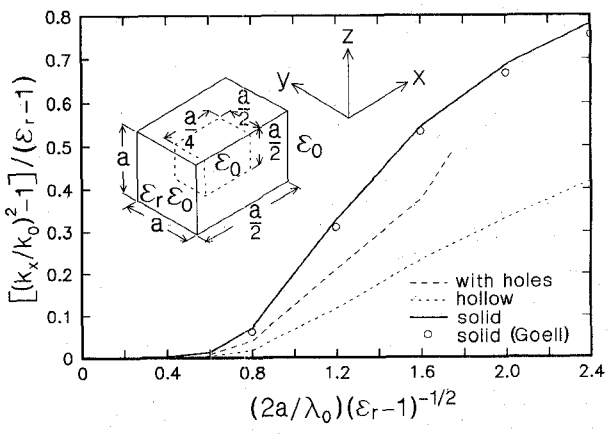

Fig. 7. Propagation constant for square dielectric waveguide with and without periodic array of holes ($d_1/a = 0.5$, $d_2/a = 10$, $\epsilon_r = 2.25$, $S_x = 4$, $S_y = 80$, $S_z = 8$).

VII. Discussion

A procedure for modeling volume polarization currents using surface currents has been explored and successfully applied to a number of representative waveguide structures. These structures represent a stringent test of the approach, since the results involve near-field quantities. Based on the numerical convergence and the generally close agreement with previously published results, the use of rooftop currents and, in particular, corner rooftop functions within dielectric volumes has been justified. Many other structures could be handled, including those composed of spatially varying or even anisotropic dielectric constants. By defining unit cells that include multiple waveguides, coupling effects can be calculated. Though only guided-wave problems were investigated here, this volume polarization formulation has also been successfully applied to source-fed and scattering problems [29].

The approach does have constraints. Structure boundaries that do not lie on a Cartesian coordinate grid would have to be approximated by steps. Because of the roughly eight to 16 grid sections per wavelength usually required for moment method solutions, the dielectric is limited to perhaps several cubic wavelengths for 3-D problems and perhaps several tens of square wavelengths for 2-D problems. This rules out analysis of structures involving dielectric half-spaces. Some difficulty was encountered, though only in purely dielectric structures, in finding a suitable starting point for the Newton search. This difficulty would become more severe if radiative structures were considered, since a suitable guess would have to include both real and imaginary parts of the propagation constant.

Because only a single type of basis function is used, the accuracy may fall short of that possible from approaches where basis functions are specifically tailored to the structure, and especially to any conductor edges that may be present. But the virtue of this approach would become apparent in a setting where solutions of engineering accuracy for a wide variety of problems might be needed. It would not be necessary to investigate the literature and develop an assortment of individual algorithms. This single approach could be used to solve a large class of two- and three-dimensional problems.

Acknowledgment

The author wishes to express his thanks to Prof. T. Sarkar and Prof. E. Arvas of Syracuse University for the in-depth conversations on volume polarization formulations. He also expresses his thanks to L. Gurel of the University of Illinois, Urbana, for providing information on the microstrip problem and to G. Kopcsay of the IBM T. J. Watson Research Center for his insights regarding the kinds of problems that could be solved using this approach.

References

[1] R. F. Harrington, *Field Computation by Moment Methods*. New York: Macmillan, 1968.

[2] J. F. Kiang, S. M. Ali, and J. A. Kong, "Propagation properties of strip lines periodically loaded with crossing strips," *IEEE Trans. Microwave Theory Tech.*, vol. 37, pp. 776–786, Apr. 1989.

[3] L. Gurel and W. C. Chew, "Guidance or resonance conditions for strips or disks embedded in homogeneous and layered media," *IEEE Trans. Microwave Theory Tech.*, vol. 36, pp. 1498–1506, Nov. 1988.

[4] S. T. Peng, T. Tamir, and H. L. Bertoni, "Theory of periodic dielectric waveguides," *IEEE Trans. Microwave Theory Tech.*, vol. MTT-23, pp. 123–133, Jan. 1975.
[5] J. E. Goell, "A circular-harmonic computer analysis of rectangular dielectric waveguides," *Bell Syst. Tech. J.*, vol. 48, pp. 2133–2160, Sept. 1969.
[6] M. Tsuji, S. Suhara, H. Shigesawa, and K. Takiyama, "Submillimeter guided-wave experiments with dielectric rib waveguides," *IEEE Trans. Microwave Theory Tech.*, vol. MTT-29, pp. 547–552, June 1981.
[7] T. Itoh, "Inverted strip dielectric waveguide for millimeter-wave integrated circuits," *IEEE Trans. Microwave Theory Tech.*, vol. MTT-24, pp. 821–827, Nov. 1976.
[8] R. Mittra, Y. Hou, and V. Jamnejad, "Analysis of open dielectric waveguides using mode-matching technique and variational methods," *IEEE Trans. Microwave Theory Tech.*, vol. MTT-28, pp. 36–43, Jan. 1980.
[9] S. M. Rao, E. Arvas, and T. K. Sarkar, "Combined field solution for TM scattering from multiple conducting and dielectric cylinders of arbitrary cross section," *IEEE Trans. Antennas Propagat.*, vol. AP-35, pp. 447–451, April 1987.
[10] E. Arvas and T. K. Sarkar, "RCS of two-dimensional structures consisting of both dielectrics and conductors of arbitrary cross section," *IEEE Trans. Antennas Propagat.*, vol. 37, pp. 546–554, May 1989.
[11] K. Umashankar, A. Taflove, and S. M. Rao, "Electromagnetic scattering by arbitrary shaped three-dimensional homogeneous lossy dielectric objects," *IEEE Trans. Antennas Propagat.*, vol. AP-34, pp. 758–766, June 1986.
[12] A. W. Glisson, "An integral equation for electromagnetic scattering from homogeneous dielectric bodies," *IEEE Trans. Antennas Propagat.*, vol. AP-32, pp. 173–175, Feb. 1984.
[13] G. W. Hohmann, "Three-dimensional induced polarization and electromagnetic modeling," *Geophys.*, vol. 40, pp. 309–324, Apr. 1975.
[14] M. J. Hagmann, O. P. Gandhi, and C. H. Durney, "Numerical calculation of electromagnetic energy deposition for a realistic model of man," *IEEE Trans. Microwave Theory Tech.*, vol. MTT-27, pp. 804–809, Sept. 1979.
[15] T. K. Sarkar, E. Arvas, and S. Ponnapalli, "Electromagnetic scattering from dielectric bodies," *IEEE Trans. Antennas Propagat.*, vol. 37, pp. 673–676, May 1989.
[16] D. H. Schaubert, D. R. Wilton, and A. W. Glisson, "A tetrahedral modeling method for electromagnetic scattering by arbitrarily shaped inhomogeneous dielectric bodies," *IEEE Trans. Antennas Propagat.*, vol. AP-32, pp. 77–85, Jan. 1984.
[17] M. F. Cátedra, E. Gago, and L. Nuño, "A numerical scheme to obtain the rcs of three-dimensional bodies of resonant size using the conjugate gradient method and the fast fourier transform," *IEEE Trans. Antennas Propagat.*, vol. 37, pp. 528–537, May 1989.
[18] R. F. Harrington and J. R. Mautz, "An impedance sheet approximation for thin dielectric shells," *IEEE Trans. Antennas Propagat.*, vol. AP-23, pp. 531–534, July 1975.
[19] J. H. Richmond, "A wire-grid model for scattering by conducting bodies," *IEEE Trans. Antennas Propagat.*, vol. AP-14, pp. 782–786, Nov. 1966.
[20] D. A. Hill and J. R. Wait, "Electromagnetic surface wave propagation over a bonded wire mesh," *IEEE Trans. Electromagn. Compat.*, vol. EMC-19, pp. 2–7, Feb. 1977.
[21] B. J. Rubin, "Full-wave analysis of waveguides involving finite-size dielectric regions," to be published in *1990 IEEE MTT-S Int. Microwave Symp. Dig.* (Dallas, TX), May 8–10, 1990.
[22] B. J. Rubin, "Electromagnetic approach for modeling high-performance computer modules," *IBM J. Res. Develop.*, to be published.
[23] B. J. Rubin, "Modeling arbitrarily shaped signal lines and discontinuities," *IEEE Trans. Microwave Theory Tech.*, vol. 37, pp. 1057–1060, June 1989.
[24] B. J. Rubin, "The propagation characteristics of signal lines in a mesh-plane environment," *IEEE Trans. Microwave Theory Tech.*, vol. MTT-32, pp. 522–531, May 1984.
[25] B. J. Rubin and H. L. Bertoni, "Waves guided by conductive strips above a periodically perforated ground plane," *IEEE Trans. Microwave Theory Tech.*, vol. MTT-31, pp. 541–549, July 1983.
[26] C. H. Chan and R. Mittra, "The propagation characteristics of signal lines embedded in a multilayered structure in the presence of a periodically perforated ground plane," *IEEE Trans. Microwave Theory Tech.*, vol. 36, pp. 968–975 June 1988.
[27] A. R. Djordjević and T. K. Sarkar, "A theorem on the moment methods," *IEEE Trans. Antennas Propagat*, vol. AP-35, pp. 353–355, Mar. 1987.
[28] J. R. Mautz and R. F. Harrington, "An *E*-field solution for a conducting surface small comparable to the wavelength," *IEEE Trans. Antennas Propagat.*, vol. AP-32, pp. 330–339, Apr. 1984.
[29] B. J. Rubin and S. Daijavad, "Radiation and scattering from structures involving finite-size dielectric regions," submitted to *IEEE Trans. Antennas Propagat.*

A Local Mesh Refinement Algorithm for the Time Domain–Finite Difference Method Using Maxwell's Curl Equations

IHN S. KIM, STUDENT MEMBER, IEEE, AND
WOLFGANG J. R. HOEFER, SENIOR MEMBER, IEEE

***Abstract*—In this paper we consider an efficient local mesh refinement algorithm subdividing a computational domain to resolve fine dimensions in a TD–FD space–time grid structure. At a discontinuous coarse–fine mesh interface, the boundary conditions for the tangential and normal field components are enforced for a smooth transition of highly nonuniform field quantities.**

I. Introduction

It is rather straightforward to model a region with smoothly varying field by using a uniform grid system of large mesh size. However, when the computational domain contains sharp discontinuities or objects, the fields become highly nonuniform in the vicinity of the discontinuities, and a mesh of very small mesh size must be employed. This requires a very extensive computational effort.

There are two ways to take into account the strong nonuniformity around a local discontinuity. The first is to use a mesh with gradually changing mesh size as it is currently employed in the TLM method. Such a procedure was introduced in the TD–FD method by Choi and Hoefer [1]. The problem with this method is that for a constant stability factor throughout the mesh, the time step Δt must always be varied in accordance with the local mesh size Δl.

In this paper, we propose an alternative approach, which was presented in more general form by Berger and Oliger [2] in 1984 for simple general hyperbolic partial differential equations. We have applied this approach specifically to Maxwell's two curl equations. In this approach we embed a locally uniform mesh of higher density into the larger mesh. The local uniformity of the mesh is important for keeping the same stability criterion during a simulation. This means that in the different subparts of the mesh, the ratio of Δt to Δl is kept the same. This has the advantage that in all subareas of the mesh exactly the same TD–FD algorithm can be employed.

Furthermore, Holland and Simpson [3] introduced the thin-strut formalism to include arbitrarily fine wires in their TD–FD code, THREDE, in 1981. Kunz and Simpson [4] also introduced an expansion approach to resolve locally fine objects. They first computed the field with a coarse mesh, thus obtaining the values of the tangential electric field at interfaces with a subsequently refined mesh area, which was analyzed in a second run.

In our approach, the coarse and the fine mesh regions are solved simultaneously, and the boundary conditions between the two regions are enforced to ensure a smooth transition of highly nonuniform field quantities. Furthermore, this scheme is recursive; that is, it can provide a finer and finer resolution if necessary.

Manuscript received September 5, 1989, revised January 15, 1990. This work was supported by the Natural Science and Engineering Research Council of Canada and by the Telecommunication Research Institute of Ontario.

The authors are with the Department of Electrical Engineering, University of Ottawa, 770 King Edward Ave., Ottawa, Ont., Canada K1N 6N5.

IEEE Log Number 9034900.